15th World Congress on Computational Mechanics (WCCM-XV)
8th Asian Pacific Congress on Computational Mechanics (APCOM-VIII)
Virtual Congress: 31 July – 5 August 2022
S. Koshizuka (Ed.)

MODELLING AND VALIDATION OF SELECTIVE LASER SINTERING OF PA12

K.MEINERT[1], M.BAYAT[1], D.PEDERSEN[1] AND J.HATTEL[1]

[1]Department of Mechanical Engineering, Technical University of Denmark
Kollediebakken 13, 2800 Kongens Lyngby
kemei@mek.dtu.dk

Key words: Selective laser sintering, Modelling, Validation, Mesh Refinement, PA12

Abstract. *One of the larger growing fields within additive manufacturing is the selective laser sintering process of semi-crystalline polymer powders. The powder is locally fused at certain areas, due to the energy output of a laser. This method allows for rapid production of complex parts, which are well suited for prototyping. The overall accuracy and stability of the process along with part properties are highly related to the process parameter. A better control of these parameters will therefore optimize the process even further. The current paper propos a numerical modelling approach and the model makes it possible, to analyze the influence of the laser-related input parameters concerning the temperature distribution and size of the melt pool. For the validation, certain outputs from the model are compared to the ones found from experimental single-line track data, where the melt pool geometry can be compared to the numerical measurements.*

1 INTRODUCTION

Selective laser sintering (**SLS**) has formerly shown to be a well-suited production method, for making rapid prototypes, complex structures and a good surface finish. Challenges however arise as the parts shape, structure and properties, among others, are strongly affected by the laser power, scan speed, hatch distance and packing densities. The parameters also affect the cooling of the part and therefore the warpage and internal stresses [1-3]. The need for better control and perception of the overall process during the manufacturing of parts is therefore highly valued. Several other studies have constructed models in order to investigate the effect of the process parameters, and changes in the melt pool geometry as these data, are hard to extract experimentally. Former methodologies have successfully computed the geometries of the melt pool and validated their model with experimental data. However, no verified methodology has been proposed, in order to develop a validated model and further testing the results by experimental measurements. [1-3]
The current paper therefore proposes and scrutinizes a more simple method for estimating the melt pool geometries sufficiently, by a numerical model. This is accomplished, by a 3-dimensional heat transfer model, with a Gaussian laser profile. The model is further supplied

with an adaptive mesh refinement and adjustable time step size algorithms, for higher accuracy where and when needed.
Everything is hardcoded in Matlab Livelink using the FEM-based commercial software package COMSOL Multiphysics.

2 EXPERIMENTAL SETUP

The experimental data utilized for validation of the model has been produced on a EOS P500 System, which is a widely used commercial available machine that is seen utilized in the industry. Figure [1] shows the basic concept of the SLS system with an Infrared camera integrated. The wavelengths of the laser, protection glass and camera is further illustrated.

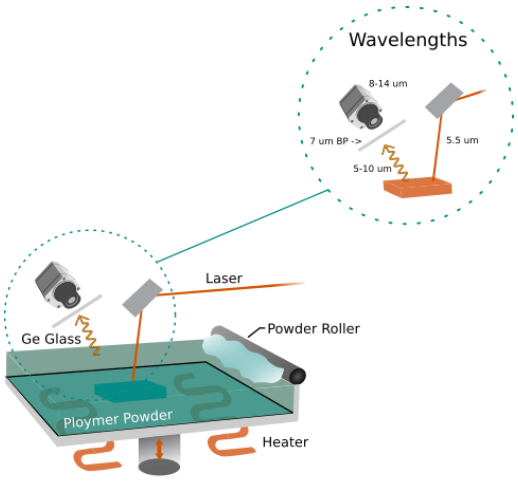

Figure 1 - Concept of SLS with integrated Camera

..

2.1 Material data

The material used in the simulation is PA12, which is a common polymer compound for the manufacturing process. The material properties, is measured from a powder mixture of 50% Reduced powder. As this is normal in the industry, the material data results serve great value.

2.1.1 Conductivity

The conductivity of the PA12 was determined experimentally. An interpolation was made, so that a continues function could be used to assign the appropriate conductivity for the powder during simulation every time step in the model.

$$\lambda(T) = 0.078 + \frac{0.23}{(1 + 10^{(20-0.12T)})} \left[\frac{W}{mK}\right] \quad (1)$$

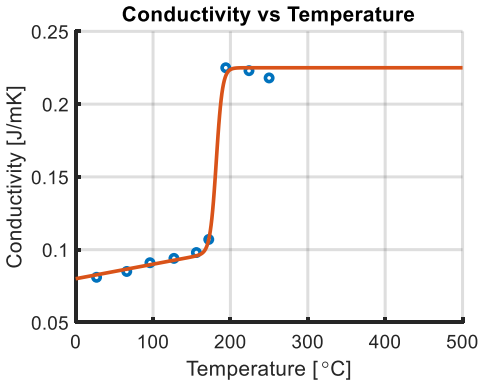

Figure 2 - Thermal conductivity as function of temperature (PA12)

2.1.2 Specific heat

The specific heat for the material, was experimentally measured. A piecewise function of three segments was then applied, in order to match the tendency. The first segment up to 190 [°C], is presented in the paper. For more information contact first author of the presented work.

$$C_p(T) = \frac{0.014301T + 1.549 + 109}{0.75 * (T - 184)^2 + 7.3} \ \epsilon \ [x < 190] \tag{2}$$

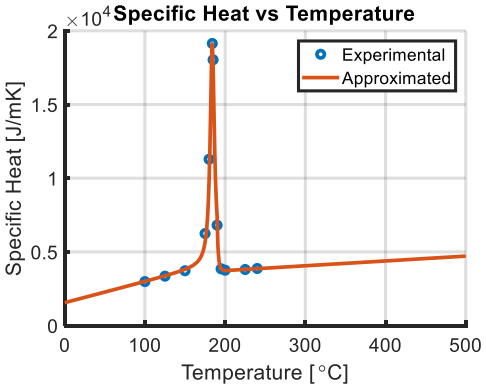

Figure 3 - Specific Heat as function of Temperature (PA12)

2.1.3 Specific heat

The coefficient of thermal expansion (**CTE**) was further measured. This property becomes interesting, when the future model is expanded to couple with mechanical analysis after the thermal simulation.

$$CTE(T) = 5e-6 * T^2 + 5e-4 - 8e-4 \ \left[\frac{m}{°C}\right] \tag{3}$$

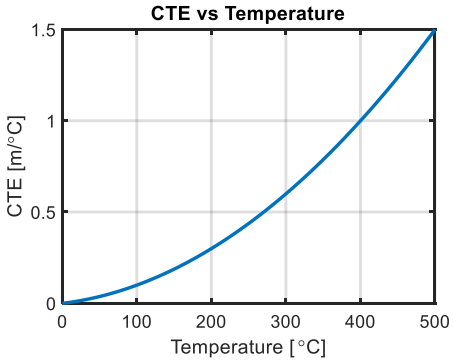

Figure 4 - Coefficient of Thermal Expansion as function of temperature (PA12)

3 METHODLOGY

The creation of the model bounded first in a 3-Dimensional conductive heat transfer model, which was then expanded to include a Gaussian distribution as heat source input. The latent heat release, which is an exothermic process, was modelled by the means of an increase in the heat capacity. A return algorithm was then implemented to ensure that this step was included if a node received higher temperature, then its temperature would be reduced slightly in order to ensure the inclusion of the exothermic process.

3.1 Conductive Heat Transfer

The conductive heat transfer in 3D, was integrated through the Alternating Direction Implicit method (**ADI**) in the Matlab model, which contains the beneficial properties of the implicit method, by being timewise unconditional stable compared to the explicit solver. The formulation is the foundation for all simulation regarding heat transfer modelling.

$$\left(\frac{\delta T}{\delta t}\right) = \alpha * \left(\frac{\delta^2 T}{\delta x^2}\right) + \left(\frac{\delta^2 T}{\delta y^2}\right) + \left(\frac{\delta^2 T}{\delta z^2}\right) \tag{3}$$

3.2 Heat source modelling

The laser profile was assumed, to follow a Gaussian distribution profile, which has formerly been shown to be a good fit for CO_2 lasers. The laser spot size was determined with a pinhole and a photodiode setup, where the pinhole could be adjusted and the intensity profile measure. Measured by an EOS technician on the P500.

$$q_{xy}(x,y) = \frac{2\eta P}{\pi r_{spot}^2} * \exp\left(\frac{-2 * (x - vt^2 + y^2}{r_{spot}^2}\right) \tag{4}$$

3.3 Adaptive Mesh Refinement (AMR)

The accuracy of the model is highly dependent on the correct mesh size densities near the melt pool geometry, as the temperature gradients here, will be most severe. In order to account for this behavior an adaptive mesh refinement was implemented in the COMSOL model. Which is automatically adjusted by an error estimator, over the thermal gradients between the mesh elements. COMSOL AMR had the possibility of both refining and ensuring the best fit between accuracy and computation time. This method was applied for all simulation.

3.4 Time step adjustment

In order to ensure that the accuracy vs computation time optimized, a time adjustment algorithm was applied in COMSOL. The algorithm ensured that the minimum time step criterion is fulfilled. This criterion can be determined from the Fourier number, and was implied as a mask indexing the smallest element, and setting the criteria from this statement. The equation is based on the Fourier number in 3D, which is the general criteria for time wise stability.

$$dt \leq \frac{3dx^2}{\frac{6\lambda}{\rho Cp}} \tag{5}$$

4 RESULTS AND DISCUSSION

The proposed model, showed great advantages being constructed in COMSOL, due to very fast computation times and ease of implementation for a variety of features and simulation loops. The Gaussian laser source profile was both implemented by a moving heat source, but also a beam deposited power feature integrated in COMSOL. Both methods showed good agreements. However, the inbuilt COMSOL feature showed advantages in the computation time. It was furthermore also possible to use the model directly from Matlab via livelink, where everything including the data extraction has been automated. In this way, it also allows the model for great possibilities regarding model expansion. The model as shown in COMSOL is presented in figure [5]

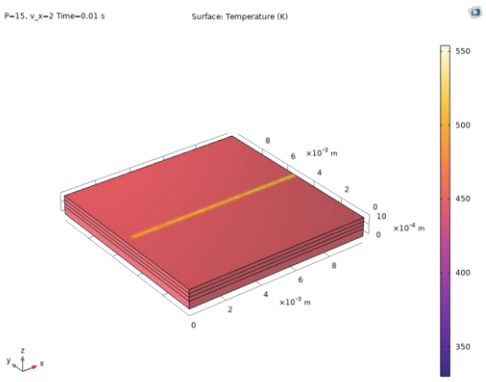

Figure 5 – COMSOL model with laser source applied

4.1 Validation

The model was validated by scan lines, that had been made on an EOS P500. The lines were enclosed in sintered boxes, so that an optimal cross-sections could be cut afterwards. After the samples were cut they were cold molded into epoxy and then grinded and polished. A development of a grinding and polishing recipe for SLS prints were made in this process. Figure [6]

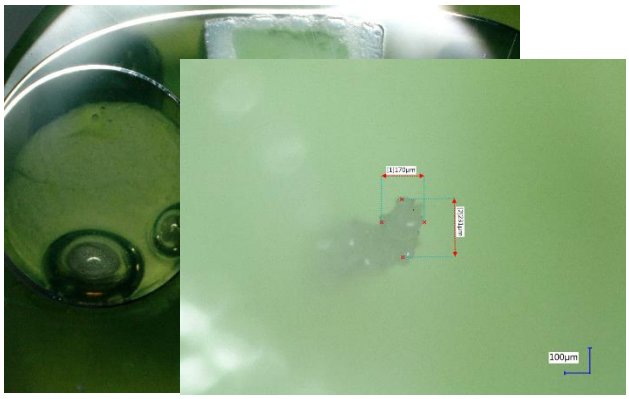

Figure 6 - LOM Measurements o the scanline

It can be observed that the model accuracy was somewhat limited, but within acceptable regimes given the standard deviation of the experimentally measured data, further validating the method for further experiments being conducted. It should also be noticed that the method was innovative and has potential for optimization giving the following model expansions and further validation studies.

Case	$D_{mes}\,(\mu)$	$\sigma_{mes}(\mu)$	$d_{sim}(\mu)$	$\varepsilon = \frac{d_{mes} - d_{sim}}{d_{mes}}(\%)$
1	309	73	325	-5
2	253	43	408	-61
3	316	51	440	-39
4	250	34	321	-28
5	236	26	389	-64
6	235	39	403	-71
7	234	51	320	-36

Tabel 1 - Experimentally measured and simulated melt pool widths

4.2 Process parameters

The melt pool width as function of the power for a fixed scan speed of 2 [m/s] is shown in figure [4]. It is clear from the results that the width, as expected, increased with increasing power. The simulation results clearly illustrates this behavior while the experimental results shows some inaccuracy from this expectation, which was also shown in the data table of the results. It was further observed, that this curve tends to follow a linear relation up to a steady state where the melt pool goes towards a plateau, which could be explained by limited absorptivity by the melt, during the exothermic process of the phase change.

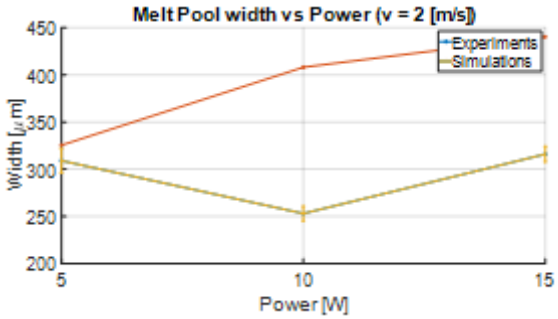

Figure 7 - Melt pool width as function of power

Examining the influence of the scan speed one see a corresponding negative relation between a higher scan speed and a decrease in melt pool width. This is also expected as the higher scan speed, will induce a lower time of the heat transfer to occour in the surface.

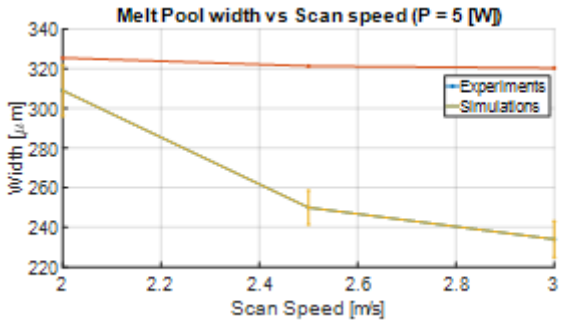

Figure 8 - Melt pool width as function of scan speed

4.3 Design of Experiments

A numerical DOE was further conducted, in order to study the effect of different power, scan speeds on the response variables. The maineffect plot for the Width and Maximum temperature are depicted in figure [6] and [7]. The two figures clearly presents, that the main influential factor for the increments of the melt pool within these parameter ranges, was the power, as expected from the process parameter analysis.

The main effect plot for the melt pool width, clearly shows that both power and scan speed has high influents on the width, with the power being the more significant factor. It is interesting to see that the scan speed has a linear relation with the melt pool width, where the power seems to go toward decreased influents as the power reaches an upper threshold.

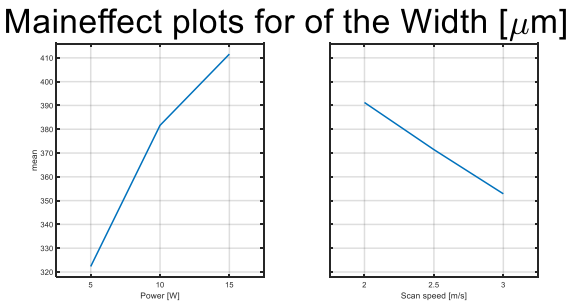

Figure 9 - Maineffect plot of the melt pool width

Investigating the maximum temperature as the response variable, figure [7] shows that the power and scan speed, are both a linear tendency, where the power again, is the main influential factor. Here as expected one can see that increasing scan speed has an inverted effect and reduces the maximum temperature detected. Compared to the melt pool width one can observe that the power obtain a higher influence for the maximum temperature at higher levels where the significant for the melt pool width is decreasing at higher levels, matching these to relations.

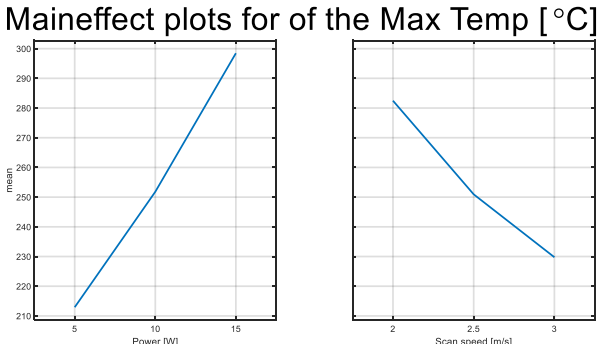

Figure 10 - Maineffect plot for the Maximum temperature

4 CONCLUSION

The model in general showed great advantages in implementation of additional features and computation time. Furthermore, it remains accessible to all academic students and researchers. The model can easily be converted into e.g. Matlab and used in all corners of the research, industry and even educational purposes.

The model included approximation for PA12 material data, which had 50% reuse powder. This is a common mixture in the industry and can be used for further analysis and future

models of similar systems to come. No results for reused powder was found within the initial literature study, showing a great advantage in filling this gap.

The Melt pool geometry was successfully measured and compared to another work conducted by Enlargen University [1]. The model showed good agreement with the tendencies of both the model from the literature and the experimental data they had acquired, but further proposed a more systematic approach for measuring scan lines.

The influence of the process parameters was, as expected, that an increase in power or decrease in scan speed, would enlarge the melt pool width. This becomes significant in the attempt of building a digital twin, which can estimate an ideal hatch distance depending on these two parameters, and furthermore set the foundation for a real-time feedback control, of the power based on threshold comparison of the melt pol geometry. Examining the results from the DOE analysis, it is evident that the most influential parameter for the melt pool geometries and maximum temperature is the power, and showed a matching tendency in significant reduction and increase between these two parameters at higher levels.

Future work will be related to refining the model and acquiring thermal images and photodiode data during single track scans from the process. While making a more comprehensive validation study, with model calibration to ensure a higher match between what is experimentally and computationally observed. Eventually a fingerprint will be made and a larger numerical DOE will be utilized to get statistical models for how the ideally control the process parameters in real time, during the manufacturing process.

REFERENCES

[1] Modelling, simulation and experimental validation of heat transfer in selective laser melting of the polymeric material PA12. D. Riedlbauer a , M. Drexler b , D. Drummer b , P. Steinmann a , J. Mergheim a,⇑

[2] Modelling of selective laser melting process with adaptive remeshing - K. Khan & A. De

[3] Process of selective laser sintering of polymer powders: Modeling, simulation, and validation. Aoulaiche Mokrane, M'hamed Boutaous ∗, Shihe Xin

[4] PROCESS MONITORING IN LASER SINTERING USING THERMAL IMAGING- A. Wegner* and G. Witt*

[5] Modeling of Laser Beam Absorption in a Polymer Powder Bed - Fuad Osmanlic 1,2,* ,†, Katrin Wudy 2,3,†, Tobias Laumer 2,4,†, Michael Schmidt 2,4 , Dietmar Drummer 2,3 and Carolin Körner 1,2,5

[6] Intelligent optimization system for powder bed fusion of processable thermoplastics - Shangqin Yuana,b, *, Jiang Lib , Xiling Yaoc , Jihong Zhua,b, *, Xiaojun Gua,b , Tong Gaoa,b , Yingjie Xua,b , Weihong Zhangb

[7] In-Situ Laser Control Method for Polymer Selective Laser Sintering (SLS) - Tim Phillips, Austin McElroy, Scott Fish, Joseph Beaman

[8] Experimental and numerical analysis of the selective laser sintering (SLS) of PA12 and PEKK semi-crystalline polymers - Patrice Peyre∗, Yann Rouchausse, Denis Defauchy, Gilles Régnier